

Search for WW and WZ Resonances Decaying to Electron, Missing E_T , and Two Jets in $p\bar{p}$ Collisions at $\sqrt{s} = 1.96$ TeV.

- T. Aaltonen,²⁵ J. Adelman,¹⁵ B. Álvarez González,^{13,x} S. Amerio,^{46,45} D. Amidei,³⁶ A. Anastassov,⁴⁰ A. Annovi,²¹
 J. Antos,¹⁶ G. Apollinari,¹⁹ J. Appel,¹⁹ A. Apresyan,⁵⁴ T. Arisawa,⁶⁵ A. Artikov,¹⁷ J. Asaadi,⁶⁰ W. Ashmanskas,¹⁹
 A. Attal,⁴ A. Aurisano,⁶⁰ F. Azfar,⁴⁴ W. Badgett,¹⁹ A. Barbaro-Galtieri,³⁰ V. E. Barnes,⁵⁴ B. A. Barnett,²⁷ P. Barria,^{51,49}
 P. Bartos,¹⁶ G. Bauer,³⁴ P.-H. Beauchemin,³⁵ F. Bedeschi,⁴⁹ D. Beecher,³² S. Behari,²⁷ G. Bellettini,^{50,49} J. Bellinger,⁶⁷
 D. Benjamin,¹⁸ A. Beretvas,¹⁹ A. Bhatti,⁵⁶ M. Binkley,^{19,a} D. Bisello,^{46,45} I. Bizjak,^{32,ee} R. E. Blair,² C. Blocker,⁸
 B. Blumenfeld,²⁷ A. Bocci,¹⁸ A. Bodek,⁵⁵ V. Boisvert,⁵⁵ D. Bortoletto,⁵⁴ J. Boudreau,⁵³ A. Boveia,¹² B. Brau,^{12,b}
 A. Bridgeman,²⁶ L. Brigliadori,^{7,6} C. Bromberg,³⁷ E. Brubaker,¹⁵ J. Budagov,¹⁷ H. S. Budd,⁵⁵ S. Budd,²⁶ K. Burkett,¹⁹
 G. Busetto,^{46,45} P. Bussey,²³ A. Buzatu,³⁵ K. L. Byrum,² S. Cabrera,^{18,z} C. Calancha,³³ S. Camarda,⁴ M. Campanelli,³²
 M. Campbell,³⁶ F. Canelli,^{15,19} A. Canepa,⁴⁸ B. Carls,²⁶ D. Carlsmith,⁶⁷ R. Carosi,⁴⁹ S. Carrillo,^{20,o} S. Carron,¹⁹
 B. Casal,¹³ M. Casarsa,¹⁹ A. Castro,^{7,6} P. Catastini,^{51,49} D. Cauz,⁶¹ V. Cavaliere,^{51,49} M. Cavalli-Sforza,⁴ A. Cerri,³⁰
 L. Cerrito,^{32,r} S. H. Chang,²⁹ Y. C. Chen,¹ M. Chertok,⁹ G. Chiarelli,⁴⁹ G. Chlachidze,¹⁹ F. Chlebana,¹⁹ K. Cho,²⁹
 D. Chokheli,¹⁷ J. P. Chou,²⁴ K. Chung,^{19,p} W. H. Chung,⁶⁷ Y. S. Chung,⁵⁵ T. Chwalek,²⁸ C. I. Ciobanu,⁴⁷ M. A. Ciocci,^{51,49}
 A. Clark,²² D. Clark,⁸ G. Compostella,⁴⁵ M. E. Convery,¹⁹ J. Conway,⁹ M. Corbo,⁴⁷ M. Cordelli,²¹ C. A. Cox,⁹ D. J. Cox,⁹
 F. Crescioli,^{50,49} C. Cuenca Almenar,⁶⁸ J. Cuevas,^{13,x} R. Culbertson,¹⁹ J. C. Cully,³⁶ D. Dagenhart,¹⁹ N. d'Ascenzo,^{47,w}
 M. Datta,¹⁹ T. Davies,²³ P. de Barbaro,⁵⁵ S. De Cecco,⁵⁷ A. Deisher,³⁰ G. De Lorenzo,⁴ M. Dell'Orso,^{50,49} C. Deluca,⁴
 L. Demortier,⁵⁶ J. Deng,^{18,g} M. Deninno,⁶ M. d'Errico,^{46,45} A. Di Canto,^{50,49} B. Di Ruzza,⁴⁹ J. R. Dittmann,⁵
 M. D'Onofrio,⁴ S. Donati,^{50,49} P. Dong,¹⁹ T. Dorigo,⁴⁵ S. Dube,⁵⁹ K. Ebina,⁶⁵ A. Elagin,⁶⁰ R. Erbacher,⁹ D. Errede,²⁶
 S. Errede,²⁶ N. Ershaidat,^{47,dd} R. Eusebi,⁶⁰ H. C. Fang,³⁰ S. Farrington,⁴⁴ W. T. Fedorko,¹⁵ R. G. Feild,⁶⁸ M. Feindt,²⁸
 J. P. Fernandez,³³ C. Ferrazza,^{52,49} R. Field,²⁰ G. Flanagan,^{54,t} R. Forrest,⁹ M. J. Frank,⁵ M. Franklin,²⁴ J. C. Freeman,¹⁹
 I. Furic,²⁰ M. Gallinaro,⁵⁶ J. Galyardt,¹⁴ F. Garberson,¹² J. E. Garcia,²² A. F. Garfinkel,⁵⁴ P. Garosi,^{51,49} H. Gerberich,²⁶
 D. Gerdes,³⁶ A. Gessler,²⁸ S. Giagu,^{58,57} V. Giakoumopoulou,³ P. Giannetti,⁴⁹ K. Gibson,⁵³ J. L. Gimmell,⁵⁵
 C. M. Ginsburg,¹⁹ N. Giokaris,³ M. Giordani,^{62,61} P. Giromini,²¹ M. Giunta,⁴⁹ G. Giurgiu,²⁷ V. Glagolev,¹⁷ D. Glenzinski,¹⁹
 M. Gold,³⁹ N. Goldschmidt,²⁰ A. Golossanov,¹⁹ G. Gomez,¹³ G. Gomez-Ceballos,³⁴ M. Goncharov,³⁴ O. González,³³
 I. Gorelov,³⁹ A. T. Goshaw,¹⁸ K. Goulianatos,⁵⁶ A. Gresele,^{46,45} S. Grinstein,⁴ C. Grossos-Pilcher,¹⁵ R. C. Group,¹⁹
 U. Grundler,²⁶ J. Guimaraes da Costa,²⁴ Z. Gunay-Unalan,³⁷ C. Haber,³⁰ S. R. Hahn,¹⁹ E. Halkiadakis,⁵⁹ B.-Y. Han,⁵⁵
 J. Y. Han,⁵⁵ F. Happacher,²¹ K. Hara,⁶³ D. Hare,⁵⁹ M. Hare,⁶⁴ R. F. Harr,⁶⁶ M. Hartz,⁵³ K. Hatakeyama,⁵ C. Hays,⁴⁴
 M. Heck,²⁸ J. Heinrich,⁴⁸ M. Herndon,⁶⁷ J. Heuser,²⁸ S. Hewamanage,⁵ D. Hidas,⁵⁹ C. S. Hill,^{12,d} D. Hirschbuehl,²⁸
 A. Hocker,¹⁹ S. Hou,¹ M. Houlden,³¹ S.-C. Hsu,³⁰ R. E. Hughes,⁴¹ M. Hurwitz,¹⁵ U. Husemann,⁶⁸ M. Hussein,³⁷
 J. Huston,³⁷ J. Incandela,¹² G. Introzzi,⁴⁹ M. Iori,^{58,57} A. Ivanov,^{9,q} E. James,¹⁹ D. Jang,¹⁴ B. Jayatilaka,¹⁸ E. J. Jeon,²⁹
 M. K. Jha,⁶ S. Jindariani,¹⁹ W. Johnson,⁹ M. Jones,⁵⁴ K. K. Joo,²⁹ S. Y. Jun,¹⁴ J. E. Jung,²⁹ T. R. Junk,¹⁹ T. Kamon,⁶⁰
 D. Kar,²⁰ P. E. Karchin,⁶⁶ Y. Kato,^{43,n} R. Kephart,¹⁹ W. Ketchum,¹⁵ J. Keung,⁴⁸ V. Khotilovich,⁶⁰ B. Kilminster,¹⁹
 D. H. Kim,²⁹ H. S. Kim,²⁹ H. W. Kim,²⁹ J. E. Kim,²⁹ M. J. Kim,²¹ S. B. Kim,²⁹ S. H. Kim,⁶³ Y. K. Kim,¹⁵ N. Kimura,⁶⁵
 L. Kirsch,⁸ S. Klimenko,²⁰ B. R. Ko,¹⁸ K. Kondo,⁶⁵ D. J. Kong,²⁹ J. Konigsberg,²⁰ A. Korytov,²⁰ A. V. Kotwal,¹⁸
 M. Kreps,²⁸ J. Kroll,⁴⁸ D. Krop,¹⁵ N. Krumnack,⁵ M. Kruse,¹⁸ V. Krutelyov,¹² T. Kuhr,²⁸ N. P. Kulkarni,⁶⁶ M. Kurata,⁶³
 S. Kwang,¹⁵ A. T. Laasanen,⁵⁴ S. Lami,⁴⁹ S. Lammel,¹⁹ M. Lancaster,³² R. L. Lander,⁹ K. Lannon,^{41,v} A. Lath,⁵⁹
 G. Latino,^{51,49} I. Lazzizzera,^{46,45} T. LeCompte,² E. Lee,⁶⁰ H. S. Lee,¹⁵ J. S. Lee,²⁹ S. W. Lee,^{60,y} S. Leone,⁴⁹ J. D. Lewis,¹⁹
 C.-J. Lin,³⁰ J. Linacre,⁴⁴ M. Lindgren,¹⁹ E. Lipeles,⁴⁸ A. Lister,²² D. O. Litvintsev,¹⁹ C. Liu,⁵³ T. Liu,¹⁹ N. S. Lockyer,⁴⁸
 A. Loginov,⁶⁸ L. Lovas,¹⁶ D. Lucchesi,^{46,45} J. Lueck,²⁸ P. Lujan,³⁰ P. Lukens,¹⁹ G. Lungu,⁵⁶ J. Lys,³⁰ R. Lysak,¹⁶
 D. MacQueen,³⁵ R. Madrak,¹⁹ K. Maeshima,¹⁹ K. Makhoul,³⁴ P. Maksimovic,²⁷ S. Malde,⁴⁴ S. Malik,³² G. Manca,^{31,f}
 A. Manousakis-Katsikakis,³ F. Margaroli,⁵⁴ C. Marino,²⁸ C. P. Marino,²⁶ A. Martin,⁶⁸ V. Martin,^{23,l} M. Martínez,⁴
 R. Martínez-Ballarín,³³ P. Mastrandrea,⁵⁷ M. Mathis,²⁷ M. E. Mattson,⁶⁶ P. Mazzanti,⁶ K. S. McFarland,⁵⁵ P. McIntyre,⁶⁰
 R. McNulty,^{31,k} A. Mehta,³¹ P. Mehtala,²⁵ A. Menzione,⁴⁹ C. Mesropian,⁵⁶ T. Miao,¹⁹ D. Mietlicki,³⁶ N. Miladinovic,⁸
 R. Miller,³⁷ C. Mills,²⁴ M. Milnik,²⁸ A. Mitra,¹ G. Mitselmakher,²⁰ H. Miyake,⁶³ S. Moed,²⁴ N. Moggi,⁶
 M. N. Mondragon,^{19,o} C. S. Moon,²⁹ R. Moore,¹⁹ M. J. Morello,⁴⁹ J. Morlock,²⁸ P. Movilla Fernandez,¹⁹ J. Mülmenstädt,³⁰
 A. Mukherjee,¹⁹ Th. Muller,²⁸ P. Murat,¹⁹ M. Mussini,^{7,6} J. Nachtman,^{19,p} Y. Nagai,⁶³ J. Naganoma,⁶³ K. Nakamura,⁶³
 I. Nakano,⁴² A. Napier,⁶⁴ J. Nett,⁶⁷ C. Neu,^{48,bb} M. S. Neubauer,²⁶ S. Neubauer,²⁸ J. Nielsen,^{30,h} L. Nodulman,²
 M. Norman,¹¹ O. Norniella,²⁶ E. Nurse,³² L. Oakes,⁴⁴ S. H. Oh,¹⁸ Y. D. Oh,²⁹ I. Oksuzian,²⁰ T. Okusawa,⁴³ R. Orava,²⁵

K. Osterberg,²⁵ S. Pagan Griso,^{46,45} C. Pagliarone,⁶¹ E. Palencia,¹⁹ V. Papadimitriou,¹⁹ A. Papaikonomou,²⁸
A. A. Paramanov,² B. Parks,⁴¹ S. Pashapour,³⁵ J. Patrick,¹⁹ G. Paulette,^{62,61} M. Paulini,¹⁴ C. Paus,³⁴ T. Peiffer,²⁸
D. E. Pellett,⁹ A. Penzo,⁶¹ T. J. Phillips,¹⁸ G. Piacentino,⁴⁹ E. Pianori,⁴⁸ L. Pinera,²⁰ K. Pitts,²⁶ C. Plager,¹⁰ L. Pondrom,⁶⁷
K. Potamianos,⁵⁴ O. Poukhov,^{17,a} F. Prokoshin,^{17,aa} A. Pronko,¹⁹ F. Ptohos,^{19,j} E. Pueschel,¹⁴ G. Punzi,^{50,49} J. Pursley,⁶⁷
J. Rademacker,^{44,d} A. Rahaman,⁵³ V. Ramakrishnan,⁶⁷ N. Ranjan,⁵⁴ I. Redondo,³³ P. Renton,⁴⁴ M. Renz,²⁸ M. Rescigno,⁵⁷
S. Richter,²⁸ F. Rimondi,^{7,6} L. Ristori,⁴⁹ A. Robson,²³ T. Rodrigo,¹³ T. Rodriguez,⁴⁸ E. Rogers,²⁶ S. Rolli,⁶⁴ R. Roser,¹⁹
M. Rossi,⁶¹ R. Rossin,¹² P. Roy,³⁵ A. Ruiz,¹³ J. Russ,¹⁴ V. Rusu,¹⁹ B. Rutherford,¹⁹ H. Saarikko,²⁵ A. Safonov,⁶⁰
W. K. Sakumoto,⁵⁵ L. Santi,^{62,61} L. Sartori,⁴⁹ K. Sato,⁶³ V. Saveliev,^{47,w} A. Savoy-Navarro,⁴⁷ P. Schlabach,¹⁹ A. Schmidt,²⁸
E. E. Schmidt,¹⁹ M. A. Schmidt,¹⁵ M. P. Schmidt,^{68,a} M. Schmitt,⁴⁰ T. Schwarz,⁹ L. Scodellaro,¹³ A. Scribano,^{51,49}
F. Scuri,⁴⁹ A. Sedov,⁵⁴ S. Seidel,³⁹ Y. Seiya,⁴³ A. Semenov,¹⁷ L. Sexton-Kennedy,¹⁹ F. Sforza,^{50,49} A. Sfyrla,²⁶
S. Z. Shalhout,⁶⁶ T. Shears,³¹ P. F. Shepard,⁵³ M. Shimojima,^{63,u} S. Shiraishi,¹⁵ M. Shochet,¹⁵ Y. Shon,⁶⁷ I. Shreyber,³⁸
A. Simonenko,¹⁷ P. Sinervo,³⁵ A. Sisakyan,¹⁷ A. J. Slaughter,¹⁹ J. Slaunwhite,⁴¹ K. Sliwa,⁶⁴ J. R. Smith,⁹ F. D. Snider,¹⁹
R. Snihur,³⁵ A. Soha,¹⁹ S. Somalwar,⁵⁹ V. Sorin,⁴ P. Squillaciotti,^{51,49} M. Stanitzki,⁶⁸ R. St. Denis,²³ B. Stelzer,³⁵
O. Stelzer-Chilton,³⁵ D. Stentz,⁴⁰ J. Strologas,³⁹ G. L. Strycker,³⁶ J. S. Suh,²⁹ A. Sukhanov,²⁰ I. Suslov,¹⁷ A. Taffard,^{26,g}
R. Takashima,⁴² Y. Takeuchi,⁶³ R. Tanaka,⁴² J. Tang,¹⁵ M. Tecchio,³⁶ P. K. Teng,¹ J. Thom,^{19,i} J. Thome,¹⁴
G. A. Thompson,²⁶ E. Thomson,⁴⁸ P. Tipton,⁶⁸ P. Ttito-Guzmán,³³ S. Tkaczyk,¹⁹ D. Toback,⁶⁰ S. Tokar,¹⁶ K. Tollefson,³⁷
T. Tomura,⁶³ D. Tonelli,¹⁹ S. Torre,²¹ D. Torretta,¹⁹ P. Totaro,^{62,61} M. Trovato,^{52,49} S.-Y. Tsai,¹ Y. Tu,⁴⁸ N. Turini,^{51,49}
F. Ukegawa,⁶³ S. Uozumi,²⁹ N. van Remortel,^{25,c} A. Varganov,³⁶ E. Vataga,^{52,49} F. Vázquez,^{20,o} G. Velev,¹⁹ C. Vellidis,³
M. Vidal,³³ I. Vila,¹³ R. Vilar,¹³ M. Vogel,³⁹ I. Volobouev,^{30,y} G. Volpi,^{50,49} P. Wagner,⁴⁸ R. G. Wagner,² R. L. Wagner,¹⁹
W. Wagner,^{28,cc} J. Wagner-Kuhr,²⁸ T. Wakisaka,⁴³ R. Wallny,¹⁰ C. Wang,¹⁸ S. M. Wang,¹ A. Warburton,³⁵ D. Waters,³²
M. Weinberger,⁶⁰ J. Weinelt,²⁸ W. C. Wester III,¹⁹ B. Whitehouse,⁶⁴ D. Whiteson,^{48,g} A. B. Wicklund,² E. Wicklund,¹⁹
S. Wilbur,¹⁵ G. Williams,³⁵ H. H. Williams,⁴⁸ P. Wilson,¹⁹ B. L. Winer,⁴¹ P. Wittich,^{19,i} S. Wolbers,¹⁹ C. Wolfe,¹⁵
H. Wolfe,⁴¹ T. Wright,³⁶ X. Wu,²² F. Würthwein,¹¹ A. Yagil,¹¹ K. Yamamoto,⁴³ J. Yamaoka,¹⁸ U. K. Yang,^{15,s} Y. C. Yang,²⁹
W. M. Yao,³⁰ G. P. Yeh,¹⁹ K. Yi,^{19,p} J. Yoh,¹⁹ K. Yorita,⁶⁵ T. Yoshida,^{43,m} G. B. Yu,¹⁸ I. Yu,²⁹ S. S. Yu,¹⁹ J. C. Yun,¹⁹
A. Zanetti,⁶¹ Y. Zeng,¹⁸ X. Zhang,²⁶ Y. Zheng,^{10,e} and S. Zucchelli^{7,6}

(CDF Collaboration)

¹Institute of Physics, Academia Sinica, Taipei, Taiwan 11529, Republic of China²Argonne National Laboratory, Argonne, Illinois 60439, USA³University of Athens, 157 71 Athens, Greece⁴Institut de Fisica d'Altes Energies, Universitat Autònoma de Barcelona, E-08193, Bellaterra (Barcelona), Spain⁵Baylor University, Waco, Texas 76798, USA⁶Istituto Nazionale di Fisica Nucleare Bologna, I-40127 Bologna, Italy⁷University of Bologna, I-40127 Bologna, Italy⁸Brandeis University, Waltham, Massachusetts 02254, USA⁹University of California, Davis, Davis, California 95616, USA¹⁰University of California, Los Angeles, Los Angeles, California 90024, USA¹¹University of California, San Diego, La Jolla, California 92093, USA¹²University of California, Santa Barbara, Santa Barbara, California 93106, USA¹³Instituto de Fisica de Cantabria, CSIC-University of Cantabria, 39005 Santander, Spain¹⁴Carnegie Mellon University, Pittsburgh, Pennsylvania 15213, USA¹⁵Enrico Fermi Institute, University of Chicago, Chicago, Illinois 60637, USA¹⁶Comenius University, 842 48 Bratislava, Slovakia; Institute of Experimental Physics, 040 01 Kosice, Slovakia¹⁷Joint Institute for Nuclear Research, RU-141980 Dubna, Russia¹⁸Duke University, Durham, North Carolina 27708, USA¹⁹Fermi National Accelerator Laboratory, Batavia, Illinois 60510, USA²⁰University of Florida, Gainesville, Florida 32611, USA²¹Laboratori Nazionali di Frascati, Istituto Nazionale di Fisica Nucleare, I-00044 Frascati, Italy²²University of Geneva, CH-1211 Geneva 4, Switzerland²³Glasgow University, Glasgow G12 8QQ, United Kingdom²⁴Harvard University, Cambridge, Massachusetts 02138, USA²⁵Division of High Energy Physics, Department of Physics, University of Helsinki and Helsinki Institute of Physics, FIN-00014, Helsinki, Finland²⁶University of Illinois, Urbana, Illinois 61801, USA

- ²⁷The Johns Hopkins University, Baltimore, Maryland 21218, USA
²⁸Institut für Experimentelle Kernphysik, Karlsruhe Institute of Technology, D-76131 Karlsruhe, Germany
²⁹Center for High Energy Physics: Kyungpook National University, Daegu 702-701, Korea;
Seoul National University, Seoul 151-742, Korea;
Sungkyunkwan University, Suwon 440-746, Korea;
Korea Institute of Science and Technology Information, Daejeon 305-806, Korea;
Chonnam National University, Gwangju 500-757, Korea;
Chonbuk National University, Jeonju 561-756, Korea
- ³⁰Ernest Orlando Lawrence Berkeley National Laboratory, Berkeley, California 94720, USA
³¹University of Liverpool, Liverpool L69 7ZE, United Kingdom
³²University College London, London WC1E 6BT, United Kingdom
- ³³Centro de Investigaciones Energeticas Medioambientales y Tecnologicas, E-28040 Madrid, Spain
³⁴Massachusetts Institute of Technology, Cambridge, Massachusetts 02139, USA
³⁵Institute of Particle Physics: McGill University, Montréal, Québec, Canada H3A 2T8;
Simon Fraser University, Burnaby, British Columbia, Canada V5A 1S6;
University of Toronto, Toronto, Ontario, Canada M5S 1A7;
and TRIUMF, Vancouver, British Columbia, Canada V6T 2A3
- ³⁶University of Michigan, Ann Arbor, Michigan 48109, USA
³⁷Michigan State University, East Lansing, Michigan 48824, USA
- ³⁸Institution for Theoretical and Experimental Physics, ITEP, Moscow 117259, Russia
³⁹University of New Mexico, Albuquerque, New Mexico 87131, USA
⁴⁰Northwestern University, Evanston, Illinois 60208, USA
⁴¹The Ohio State University, Columbus, Ohio 43210, USA
⁴²Okayama University, Okayama 700-8530, Japan
⁴³Osaka City University, Osaka 588, Japan
⁴⁴University of Oxford, Oxford OX1 3RH, United Kingdom
- ⁴⁵Istituto Nazionale di Fisica Nucleare, Sezione di Padova-Trento, I-35131 Padova, Italy
⁴⁶University of Padova, I-35131 Padova, Italy
⁴⁷LPNHE, Université Pierre et Marie Curie/IN2P3-CNRS, UMR7585, Paris, F-75252 France
⁴⁸University of Pennsylvania, Philadelphia, Pennsylvania 19104, USA
⁴⁹Istituto Nazionale di Fisica Nucleare Pisa, I-56127 Pisa, Italy
⁵⁰University of Pisa, I-56127 Pisa, Italy
⁵¹University of Siena, I-56127 Pisa, Italy
⁵²Scuola Normale Superiore, I-56127 Pisa, Italy
- ⁵³University of Pittsburgh, Pittsburgh, Pennsylvania 15260, USA
⁵⁴Purdue University, West Lafayette, Indiana 47907, USA
⁵⁵University of Rochester, Rochester, New York 14627, USA
⁵⁶The Rockefeller University, New York, New York 10021, USA
- ⁵⁷Istituto Nazionale di Fisica Nucleare, Sezione di Roma 1, I-00185 Roma, Italy
⁵⁸Sapienza Università di Roma, I-00185 Roma, Italy
⁵⁹Rutgers University, Piscataway, New Jersey 08855, USA
⁶⁰Texas A&M University, College Station, Texas 77843, USA
⁶¹Istituto Nazionale di Fisica Nucleare Trieste/Udine, I-34100 Trieste, Italy
⁶²University of Trieste/Udine, I-33100 Udine, Italy
⁶³University of Tsukuba, Tsukuba, Ibaraki 305, Japan
⁶⁴Tufts University, Medford, Massachusetts 02155, USA
⁶⁵Waseda University, Tokyo 169, Japan
⁶⁶Wayne State University, Detroit, Michigan 48201, USA
⁶⁷University of Wisconsin, Madison, Wisconsin 53706, USA
⁶⁸Yale University, New Haven, Connecticut 06520, USA

(Received 29 April 2010; published 17 June 2010)

Using data from 2.9 fb^{-1} of integrated luminosity collected with the CDF II detector at the Tevatron, we search for resonances decaying into a pair of on-shell gauge bosons, WW or WZ , where one W decays into an electron and a neutrino, and the other boson decays into two jets. We observed no statistically significant excess above the expected standard model background, and we set cross section limits at 95% confidence level on G^* (Randall-Sundrum graviton), Z' , and W' bosons. By comparing these limits to theoretical cross sections, mass exclusion regions for the three particles are derived. The mass exclusion regions for Z' and W' are further evaluated as a function of their gauge coupling strength.

Some models of new physics beyond the standard model predict particles that decay into pairs of on-shell bosons, for example Z' , W' [1], or the Randall-Sundrum graviton G^* [2]. Searches for these particles in different decay channels have been reported elsewhere [3–9]. Most of them used final states consisting of only leptons or photons. In this Letter we search for these particles in the form of diboson resonances where one boson is a W decaying into an electron and a neutrino, and the other is a W or Z which decays into two jets. This search has the advantage of detecting two types of diboson resonances, WW and WZ , with the same final-state topology. The hadronic decay mode of the W or Z to two jets has a higher branching fraction compared to the leptonic mode; however, the background from jets also increases. Thus we implement a selection based on transverse energy (E_T) [10] of the detected objects in the final state to reduce standard model backgrounds and enhance sensitivity.

The diboson decay modes of Z' and W' directly probe the gauge coupling strength between the new and the standard model gauge bosons. The coupling strength strongly influences the decay branching ratios and the natural widths of the new gauge bosons. In an extended gauge model theory [1] the standard model coupling strength, $g \cos\theta_w$, is replaced by $\xi g \cos\theta_w$, where $\xi = C(M_W/M_V)^2$, C is a parameter that sets the coupling strength, and M_V is the mass of the new gauge boson, Z' or W' . We set cross section limits on Z' and W' as a function of mass and of ξ . Our results extend the sensitivity beyond the CDF Run I W' results [11] with almost 30 times the integrated luminosity, and, for the first time, set Z' limits as a function of mass and gauge coupling strength. For G^* , the coupling constant k/\bar{M}_{Pl} dictates the branching ratio and natural width [2], where k and \bar{M}_{Pl} are, respectively, the curvature of the extra dimension and the reduced Planck mass scale. This is also the first search for the G^* in the WW decay mode.

This analysis is based on data corresponding to an integrated luminosity of 2.9 fb^{-1} collected using the CDF II detector between March 2002 and February 2008. The detector is approximately forward-backward and azimuthally symmetric. The detector elements relevant to this analysis are the tracking system and the calorimeters. The tracking system consists of an eight-layer silicon tracker [12] surrounded by a 96-layer open-cell drift chamber (COT) [13]. The fiducial coverage of the COT is $|\eta| < 1.0$ [10], and the silicon detector extends the coverage to $|\eta| < 2.0$. The integrated tracking system is contained within a superconducting solenoid, providing a 1.4 T magnetic field. Surrounding the tracking system are the electromagnetic (EM) and hadronic calorimeters [14], divided into “central” ($|\eta| < 1.1$) and “plug” ($1.1 < |\eta| < 3.6$) regions. The calorimeters are made of lead (EM) and iron (hadronic) absorbers sandwiched between plastic scintillators that provide measurements of shower energies. At

approximately the shower maximum, the EM calorimeters contain fine-grained detectors [15] for measuring shower positions and profiles.

As we are looking for events with an electron, a neutrino, and two jets, we start with data that were collected with an online selection requirement of a central electron with $|\eta| < 1$ and $E_T > 18 \text{ GeV}$. From this data set we select events that have an isolated electron [16] with $E_T > 30 \text{ GeV}$, a neutrino identified by the requirement that the missing $E_T(\not{\!E}_T) > 30 \text{ GeV}$, two or three jets with $|\eta| < 2.5$ and $E_T > 30 \text{ GeV}$, and an overall $H_T > 150 \text{ GeV}$, where H_T is the scalar sum of the electron E_T , the $\not{\!E}_T$, and the E_T of all jets [17].

To form a WW or WZ hypothesis for the selected events, the electron and $\not{\!E}_T$ are first combined to form a W candidate. Because the longitudinal component of the neutrino momentum (E_z^ν) is not available, the invariant mass of the electron and $\not{\!E}_T$ is artificially set to the W mass. With this assumption, the conservation of energy and momentum results in a quadratic equation for E_z^ν . If the discriminant of the quadratic equation is negative, the combination is discarded. If it is positive, there are two solutions and both are kept. In addition, two jets are combined to form a second W candidate or a Z candidate. In the case of a W candidate, we require the two-jet invariant mass (M_{jj}) to fall between 65 and $95 \text{ GeV}/c^2$, corresponding to $\pm 1.5\sigma$ of the expected reconstructed W resolution. In the case of a Z candidate, this window is between 75 and $105 \text{ GeV}/c^2$. For a three-jet event, there are three two-jet invariant mass combinations. In this case only the pair with the invariant mass closest to either the W or the Z mass is kept in order to reduce the combinatorial background. The reconstructed W or Z candidates are then combined to form the final WW or WZ invariant mass.

Twelve standard model processes are considered as background for this analysis: $W(\rightarrow e^\pm \nu) + \text{jets}$, QCD jets, $t\bar{t}$, WW , $Z(\rightarrow e^+ e^-) + \text{jets}$, $W(\rightarrow \tau^\pm \nu) + \text{jets}$, single top, WZ , $W\gamma$, $Z \rightarrow \tau^+\tau^-$, $\gamma\gamma$, and ZZ . The dominating background is $W + \text{jets}$ whose contribution is estimated by Monte Carlo simulation using the ALPGEN [18] event generator, interfaced to PYTHIA [19] for parton showering and followed by the GEANT 3 [20] based CDF II detector simulation. With the exception of the QCD jet background, the rest of the background processes are all estimated by Monte Carlo simulation using the PYTHIA event generator. The cross sections used for the simulated background processes are obtained from next-to-leading order (NLO) calculations.

The QCD jet background comes from events with three or more jets where one of the jets is misidentified as an electron. With this misidentified electron, the event may pass through subsequent event selection criteria and the reconstruction processes. The contribution of the QCD jet background is estimated using a data set that has an online selection requirement of one jet with $E_T > 20 \text{ GeV}$. We

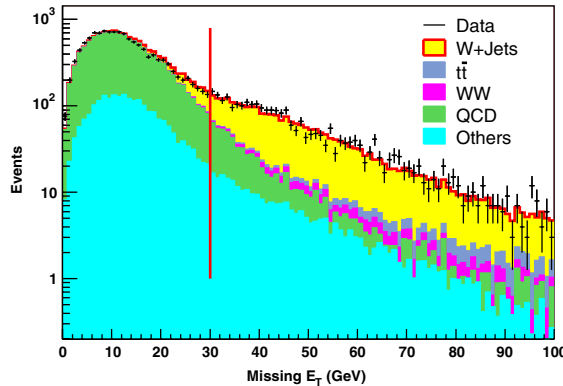


FIG. 1 (color online). \cancel{E}_T spectrum from events with an electron and two jets. The vertical line marks the $\cancel{E}_T > 30$ GeV cut. The QCD component is scaled such that data and expected background match at the peak area where no signal is expected. “Others” background includes: $Z \rightarrow e^+ e^-$ + jets, single top, WZ , $W\gamma$, $Z \rightarrow \tau^+ \tau^-$, $\gamma\gamma$, and ZZ .

first exclude events that have any identified electrons, then each jet in the central region is treated as an electron with a weight corresponding to the probability that a jet is misidentified as an electron. This probability is a function of jet E_T and varies from 10^{-4} at 30 GeV to 10^{-3} above 100 GeV [6]. The misidentified electron is combined with the \cancel{E}_T and then with two jets to form WW or WZ candidates as described earlier. The resulting QCD jet background is normalized to the data by matching the \cancel{E}_T spectrum between data and expected background at their peaks around 10 GeV, where little signal is expected and the QCD jet background dominates. This normalization factor is used for the QCD jet contribution throughout the analysis. Figure 1 shows the resulting \cancel{E}_T spectrum for events with an electron and two jets that would have passed the event selection criteria except for the $\cancel{E}_T > 30$ GeV cut.

The systematic uncertainties taken into account in the background calculations are the following, listed by decreasing significance: jet energy scale (JES) uncertainty

[21], theoretical cross section uncertainty [22], luminosity uncertainty [23], and jet misidentification rate uncertainty. The dominating systematic uncertainty is the JES uncertainty which amounts to $\sim 13\%$ of the estimated background. The cross section and luminosity uncertainties are $\sim 6\%$ each.

Signal detection efficiencies are also determined from simulated events using the PYTHIA event generator. For a set of selected mass values ranging from $165 \text{ GeV}/c^2$ to $1000 \text{ GeV}/c^2$, the three types of particles are simulated: G^* with $k/\bar{M}_{\text{Pl}} = 0.1$, Z' and W' with PYTHIA default settings corresponding to the extended gauge model with a suppression factor $\xi = (M_W/M_V)^2$, i.e., $C = 1$. The reconstructed signals are Gaussian in shape, and the mass resolution is linearly proportional to the generated mass values, varying from $20 \text{ GeV}/c^2$ at $200 \text{ GeV}/c^2$ mass to $80 \text{ GeV}/c^2$ at $1000 \text{ GeV}/c^2$ mass. For calculating the efficiencies we choose an acceptance mass window corresponding to ± 1.5 times the reconstructed signal resolution. This choice gives a good signal to background ratio. The same acceptance mass windows are also used to obtain the number of background events.

The systematic uncertainties taken into account for the signal acceptance, defined as the product of signal detection efficiency and integrated luminosity, in order of decreasing significance, are: jet energy scale (JES) uncertainty, luminosity uncertainty, initial state radiation (ISR) uncertainty, final state radiation (FSR) uncertainty, and parton distribution function (PDF) uncertainty. Similarly to the background uncertainties, the JES uncertainty dominates the systematic uncertainties and varies from 12% at $170 \text{ GeV}/c^2$ mass to 6% at $700 \text{ GeV}/c^2$ mass for G^* , 13% ($170 \text{ GeV}/c^2$) to 6% ($1000 \text{ GeV}/c^2$) for Z' , and 9% ($190 \text{ GeV}/c^2$) to 6% ($1000 \text{ GeV}/c^2$) for W' . ISR, FSR and PDF uncertainties are of the order of 1%–3% each and decrease with increasing diboson mass.

In order to improve sensitivity at higher mass, additional sets of higher E_T cuts for the constituent particles (observed in the detector as electron, \cancel{E}_T from neutrino, and jets) are tried. Two series of the E_T cut sets are imple-

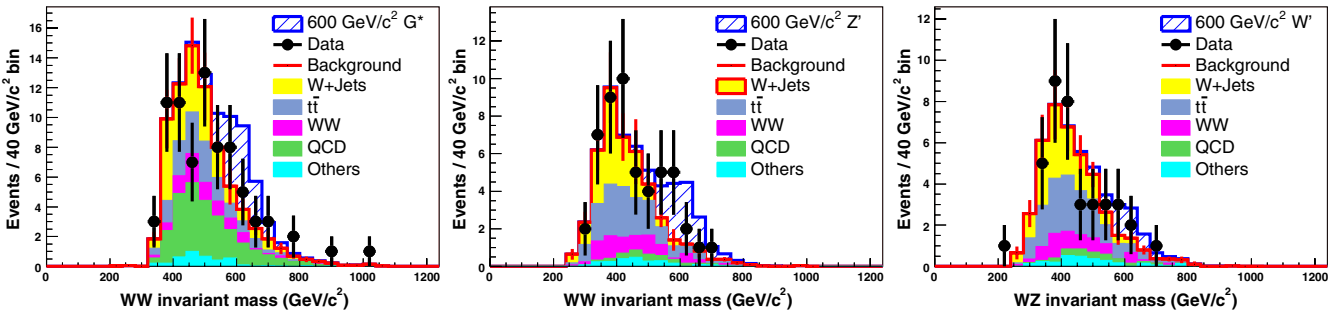


FIG. 2 (color online). Invariant mass distributions with optimal set of E_T cuts for $600 \text{ GeV}/c^2$ signals superimposed on the backgrounds. Left to right: $G^*(WW)$, $Z'(WW)$, $W'(WZ)$. G^* and Z' are the same decay mode (WW) but with different optimal selections. Z' and W' have the same optimal selection but different decay modes (WW vs WZ). The $600 \text{ GeV}/c^2$ mass signals shown correspond to the expected theoretical cross sections.

TABLE I. Percentage fractional background compositions in Fig. 2. The uncertainties include both statistical and systematic uncertainties.

	$G^*(WW)$	$Z'(WW)$	$W'(WZ)$
$W + \text{jets}$	31.8 ± 8.2	33.0 ± 10.0	36.8 ± 9.7
$t\bar{t}$	19.6 ± 2.7	35.1 ± 4.0	37.4 ± 5.2
WW	10.7 ± 3.2	15.2 ± 2.8	13.4 ± 3.2
QCD jets	32.7 ± 6.5	5.1 ± 1.0	5.6 ± 1.1
Others	5.3 ± 0.9	2.4 ± 0.9	3.4 ± 1.0

mented. The first series requires a higher E_T on all four participating particles ranging from 40 GeV to 80 GeV in steps of 10 GeV. The second series requires a higher E_T on only one daughter particle from each of the decaying bosons, i.e., a higher E_T for either the electron or the neutrino, and the same higher E_T for one of the two jets. The E_T values in this series range from 40 GeV to 120 GeV in steps of 10 GeV. For each set of E_T cuts the systematic uncertainties for the backgrounds and the acceptances are reevaluated, but are found to be not very sensitive to the variations.

To find the optimal set of E_T cuts at each selected mass point, the expected cross section limits, which are based only on the background and the signal acceptance, are calculated for each set of cuts. We found that the first series of E_T cuts gives the best expected limits for Z' and W' , while the second series is best for G^* . The optimal E_T cuts for each particle type are then selected from their own optimal series. The sets that give the best expected limits are chosen without reference to their impact on the data sample. Although the background processes respond differently to the two series of E_T cuts, the best expected limits obtained from each series are very similar. Generally, as the mass increases the higher E_T cuts yield better expected limits.

We use a Bayesian method [24] to calculate cross section limits. Inputs to the calculation are signal acceptance, estimated background, and observed data. The signal acceptance and background are assigned priors and modeled via a Monte Carlo method that allows correlation of un-

TABLE II. Mass exclusion region at 95% C.L. with $k/\tilde{M}_{\text{Pl}} = 0.1$ for G^* , and $\xi = (M_W/M_V)^2$ ($C = 1$) for Z' and W' .

	G^*	Z'	W'
Expected Exclusion (GeV/c^2)	<632	257–630	381–421
Observed Exclusion (GeV/c^2)	<607	247–544	285–516

certainties between acceptance and background. In our analysis, the JES and luminosity uncertainties in the acceptance and in the background are correlated. The expected limits are calculated by simulating observed data based on the expected background with Poisson fluctuations.

Figure 2 shows typical invariant mass distributions reconstructed for each particle type for a mass of 600 GeV/c^2 using the optimal set of E_T cuts in each case. The WW invariant mass distributions are shown for G^* and Z' , and the WZ invariant mass distribution is shown for W' . The optimal set of E_T cuts for G^* at 600 GeV/c^2 is from the second series with $E_T > 120$ GeV, while both Z' and W' favor the first series with $E_T > 60$ GeV. The background compositions, as shown in Table I, are found to be more sensitive to the different sets of E_T cuts than to the different decay types (WW or WZ). For Z' and W' , the QCD jet background has a much lower contribution owing to the stricter E_T requirements.

Without a statistically significant excess above the expected background in the invariant mass plots, we calculate the cross section limits at 95% confidence level (C.L.) for the observed data. Figure 3 shows the observed and the expected 95% C.L. cross section limits overlaid with theoretical cross sections. The theoretical cross sections for G^* and Z' are calculated from PYTHIA version 6.216, and a constant K factor of 1.3 is applied to take into account the NLO correction [4–6]. The theoretical cross section for W' is derived from a NLO calculation [25]. The upper right inserts in Fig. 3 show ratios of the limits to the theoretical cross sections. Where the ratio is below one the mass region is excluded. Table II summarizes the mass exclusion regions from the figures.

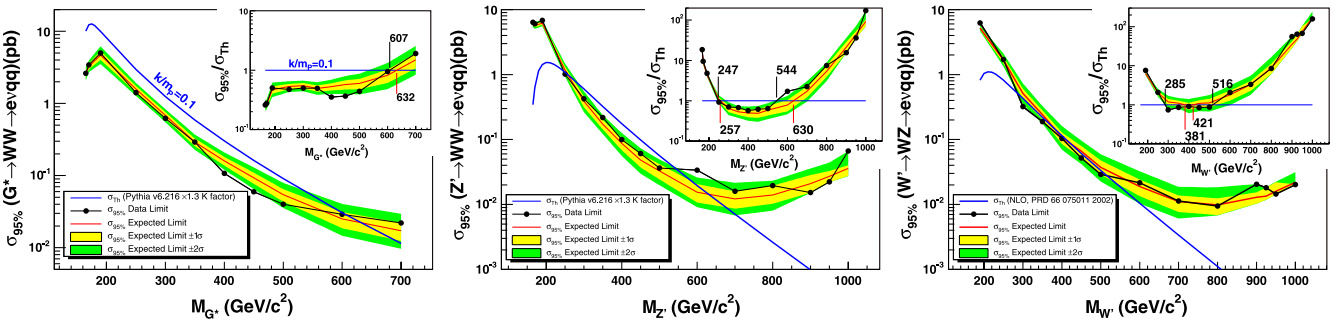


FIG. 3 (color online). Cross section limits at 95% C.L. Left to right: G^* , Z' , W' . Inserts at upper right are cross section limits divided by the theoretical cross sections. The 1σ and 2σ bands are shown for the expected limits.

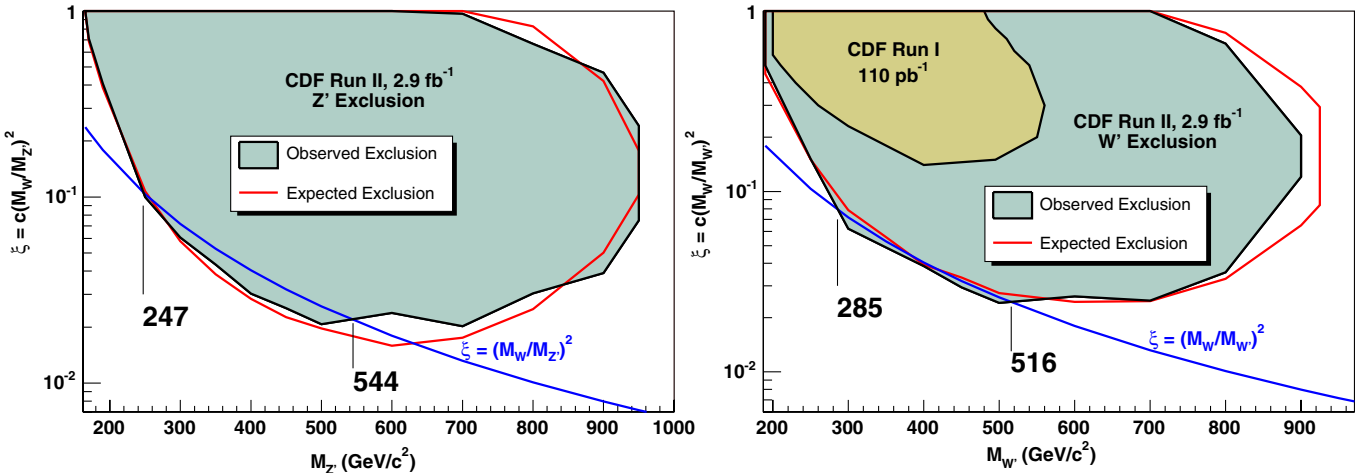


FIG. 4 (color online). Z' (left) and W' (right) exclusion regions as a function of mass and ξ . The $\xi = (M_W/M_V)^2$ (i.e., $C = 1$) lines indicate PYTHIA defaults and are commonly used for mass exclusion regions. The vertical lines mark the results as shown in Table II. Also shown in the W' plot is the CDF Run I result.

The results shown in Fig. 3 and Table II for Z' and W' are based on a gauge coupling mixing factor of $\xi = C(M_W/M_V)^2$, with $C = 1$. Since signal acceptance is the only quantity that changes with ξ in the cross section limit calculation, at each mass point we reevaluate signal acceptances for different ξ values and calculate cross section limits as a function of ξ . Comparing the calculated and theoretical cross sections as a function of ξ , a ξ exclusion region is derived at each mass point. These Z' and W' exclusion regions are shown in Fig. 4. The branching ratio of Z' or W' to fermions decreases as ξ increases. This is opposite to the diboson decay modes where branching ratios increase as ξ increases. Most Z' or W' search results [6,7] report mass limits along the $\xi = (M_W/M_V)^2$ line and we have also done so for comparison. However, the diboson decay modes and the fermionic decay modes are sensitive to different parts of the gauge coupling strength phase space, so searches for bosonic and fermionic decays of Z' and W' are complementary to each other. The W' result shown in Fig. 4 is significantly improved compared to the previous result from CDF Run I [11]. The Z' result shown is the first to set an exclusion region as a function of ξ and mass.

In conclusion, we have searched for new particles decaying into a pair of bosons in the electron, \not{E}_T , and two jets final state. In data from an integrated luminosity of 2.9 fb^{-1} , no significant excess over the standard model prediction is observed. Cross section limits at 95% C.L. and mass exclusion regions have been obtained for a Randall-Sundrum graviton, Z' and W' bosons. The W' exclusion region in the $\xi - M_{W'}$ plane has been extended significantly compared to the previous measurement. We have also presented the Z' exclusion region in the $\xi - M_{Z'}$ plane for the first time. We set the most stringent mass limits on W' and Z' bosons.

We thank the Fermilab staff and the technical staffs of the participating institutions for their vital contributions. This work was supported by the U.S. Department of Energy and National Science Foundation; the Italian Istituto Nazionale di Fisica Nucleare; the Ministry of Education, Culture, Sports, Science and Technology of Japan; the Natural Sciences and Engineering Research Council of Canada; the National Science Council of the Republic of China; the Swiss National Science Foundation; the A.P. Sloan Foundation; the Bundesministerium für Bildung und Forschung, Germany; the World Class University Program, the National Research Foundation of Korea; the Science and Technology Facilities Council and the Royal Society, UK; the Institut National de Physique Nucléaire et Physique des Particules/CNRS; the Russian Foundation for Basic Research; the Ministerio de Ciencia e Innovación, and Programa Consolider-Ingenio 2010, Spain; the Slovak R&D Agency; and the Academy of Finland.

^aDeceased

^bVisitor from University of Massachusetts Amherst, Amherst, MA 01003, USA.

^cVisitor from Universiteit Antwerpen, B-2610 Antwerp, Belgium.

^dVisitor from University of Bristol, Bristol BS8 1TL, United Kingdom.

^eVisitor from Chinese Academy of Sciences, Beijing 100864, China.

^fVisitor from Istituto Nazionale di Fisica Nucleare, Sezione di Cagliari, 09042 Monserrato (Cagliari), Italy.

^gVisitor from University of California Irvine, Irvine, CA 92697, USA.

- ^hVisitor from University of California Santa Cruz, Santa Cruz, CA 95064, USA.
- ⁱVisitor from Cornell University, Ithaca, NY 14853, USA.
- ^jVisitor from University of Cyprus, Nicosia CY-1678, Cyprus.
- ^kVisitor from University College Dublin, Dublin 4, Ireland.
- ^lVisitor from University of Edinburgh, Edinburgh EH9 3JZ, United Kingdom.
- ^mVisitor from University of Fukui, Fukui City, Fukui Prefecture, Japan 910-0017.
- ⁿVisitor from Kinki University, Higashi-Osaka City, Japan 577-8502.
- ^oVisitor from Universidad Iberoamericana, Mexico D.F., Mexico.
- ^pVisitor from University of Iowa, Iowa City, IA 52242, USA.
- ^qVisitor from Kansas State University, Manhattan, KS 66506, USA.
- ^rVisitor from Queen Mary, University of London, London, E1 4NS, United Kingdom.
- ^sVisitor from University of Manchester, Manchester M13 9PL, United Kingdom.
- ^tVisitor from Muons, Inc., Batavia, IL 60510, USA.
- ^uVisitor from Nagasaki Institute of Applied Science, Nagasaki, Japan.
- ^vVisitor from University of Notre Dame, Notre Dame, IN 46556, USA.
- ^wVisitor from Obninsk State University, Obninsk, Russia.
- ^xVisitor from University de Oviedo, E-33007 Oviedo, Spain.
- ^yVisitor from Texas Tech University, Lubbock, TX 79609, USA.
- ^zVisitor from IFIC(CSIC-Universitat de Valencia), 56071 Valencia, Spain.
- ^{aa}Visitor from Universidad Tecnica Federico Santa Maria, 110v Valparaiso, Chile.
- ^{bb}Visitor from University of Virginia, Charlottesville, VA 22906, USA.
- ^{cc}Visitor from Bergische Universität Wuppertal, 42097 Wuppertal, Germany
- ^{dd}Visitor from Yarmouk University, Irbid 211-63, Jordan.
- ^{ee}Visitor from On leave from J. Stefan Institute, Ljubljana, Slovenia.
- [1] G. Altarelli, B. Mele, and M. Ruiz-Altaba, *Z. Phys. C* **45**, 109 (1989).
- [2] L. Randall and R. Sundrum, *Phys. Rev. Lett.* **83**, 3370 (1999).
- [3] J. Alcaraz *et al.* (ALEPH, DELPHI, L3, OPAL Collaborations, LEP Electroweak Working Group), *arXiv:hep-ex/0612034v2*.
- [4] T. Aaltonen *et al.* (CDF collaboration), *Phys. Rev. Lett.* **99**, 171801 (2007).

- [5] T. Aaltonen *et al.* (CDF collaboration), *Phys. Rev. Lett.* **99**, 171802 (2007).
- [6] T. Aaltonen *et al.* (CDF collaboration), *Phys. Rev. Lett.* **102**, 031801 (2009).
- [7] V. M. Abazov *et al.* (D0 collaboration), *Phys. Rev. Lett.* **100**, 031804 (2008).
- [8] T. Aaltonen *et al.* (CDF collaboration), *Phys. Rev. Lett.* **103**, 041801 (2009); V. M. Abazov *et al.* (D0 collaboration), *Phys. Rev. Lett.* **100**, 211803 (2008).
- [9] V. M. Abazov *et al.* (D0 collaboration), *Phys. Rev. Lett.* **104**, 061801 (2010).
- [10] D. Acosta *et al.*, *Phys. Rev. D* **71**, 032001 (2005). CDF uses a cylindrical coordinate system in which $+z$ points along the direction of the proton beam, r is the radius from the nominal beam line, and ϕ is the azimuthal angle. The pseudorapidity is defined as $\eta = -\ln[\tan(\theta/2)]$, where θ is the polar angle measured from the $+z$ axis. Transverse energy is defined as $E_T = E \cdot \sin\theta$, where E is the measured calorimeter energy. Transverse momentum is defined as $p_T = p \cdot \sin\theta$, with p being the track momentum.
- [11] T. Affolder *et al.* (CDF collaboration), *Phys. Rev. Lett.* **88**, 071806 (2002).
- [12] A. Sill *et al.*, *Nucl. Instrum. Methods Phys. Res., Sect. A* **447**, 1 (2000).
- [13] T. Affolder *et al.*, *Nucl. Instrum. Methods Phys. Res., Sect. A* **526**, 249 (2004).
- [14] L. Balka *et al.*, *Nucl. Instrum. Methods Phys. Res., Sect. A* **267**, 272 (1988); S. Bertolucci *et al.*, *Nucl. Instrum. Methods Phys. Res., Sect. A* **267**, 301 (1988); M. Albrow *et al.*, *Nucl. Instrum. Methods Phys. Res., Sect. A* **480**, 524 (2002).
- [15] G. Apollinari *et al.*, *Nucl. Instrum. Methods Phys. Res., Sect. A* **412**, 515 (1998).
- [16] Electrons are isolated if in a surrounding cone of 0.4 radius the E_T deposited is no more than 1.1 times the electron E_T in the EM calorimeters.
- [17] F. Abe *et al.* (CDF collaboration), *Phys. Rev. Lett.* **75**, 3997 (1995).
- [18] Michelangelo L. Mangano *et al.*, *J. High Energy Phys.* **07** (2003) 001.
- [19] T. Sjostrand *et al.*, *Comput. Phys. Commun.* **135**, 238 (2001).
- [20] S. Agostinelli *et al.*, *Nucl. Instrum. Methods Phys. Res., Sect. A* **506**, 250 (2003).
- [21] A. Bhatti *et al.*, *Nucl. Instrum. Methods Phys. Res., Sect. A* **566**, 375 (2006).
- [22] U. Baur, T. Han, and J. Ohnemus, *Phys. Rev. D* **48**, 5140 (1993); J. M. Campbell and R. K. Ellis, *Phys. Rev. D* **60**, 113006 (1999).
- [23] D. Acosta *et al.*, *Nucl. Instrum. Methods Phys. Res., Sect. A* **494**, 57 (2002).
- [24] J. Heinrich *et al.*, *arXiv:physics/0409129*.
- [25] Z. Sullivan, *Phys. Rev. D* **66**, 075011 (2002).